Preparation of In X (X = P, As, Sb) Thin Films by Electrochemical Methods

J. Ortega and J. Herrero*

Instituto de Energias Renovables, CIEMAT, Avda. complutense, 22, E-28040 Madrid, Spain

Compounds of the III-V semiconductor family are widely used as photovoltaic detectors, optical recording materials, in semiconductor superlattice structures, etc. Also, many stable compounds of this group of semiconductor materials have been proposed as candidates for efficient solar energy conversion in solid-state photovoltaic or photoelectrochemical devices (1-2), where GaAs and InP present the most impressive solar conversion performance and stability (3-4). As III-V compound semiconductor device technology is advanced, it becomes desirable to apply some of the electrochemical preparation and characterization techniques which have proven useful for the preparation of II-VI semiconductors (5-7). While photoelectrochemical techniques have been used to characterize III-V semiconductors (8-9), few details have been published about their electrochemical preparation. GaP, InP, and GaAs have been electrodeposited from fused salt (10). In-Sb alloys have been deposited from a variety of electrolytes (11), but there is little information on electrodeposition of In-As compounds.

We have demonstrated previously that it is possible to obtain In_2Se_3 and In_2S_3 from electroplated metallic indium films by solid-phase or gas-phase chalcogenization at high temperatures (12-13). In this paper we present results on both the electrodeposition of In-Sb and In-As alloys that can be converted to crystalline, well-defined phases of InSb and InAs, and also on the formation of InP thin films by a phosphorization treatment of electroplated metallic indium films.

Experimental

All the samples were electrodeposited on titanium substrates. These strips of area 2 cm^2 and 0.3 mm thickness were polished with emery paper, cleaned with distilled water, degreased, and etched (12-13). The thicknesses of the electrodeposited films were estimated by coulometric measurements and by weighing the deposits.

Indium phosphide samples were prepared by phosphorization of electrodeposited indium thin films (13). Titanium electrodes with electrodeposited indium layers were inserted in a Pyrex tube which contained 50-100 mg of red phosphorus (Fig. 1). The tube was first evacuated to a moderate vacuum (0.01 mm Hg), sealed with Bunsen flame, then placed in a muffle furnace and heated. A heat-treatment at 130°C for at least 1h was necessary in order to avoid indium globule formation. After this pretreatment, the samples were heated for about 3h at 400°C and subsequently cooled to room temperature.

Further characterization of the thin films was accomplished by x-ray diffraction (Philips Electronics) with CuKα radiation and a Ni filter. Determination of the sample stoichiometry was performed by atomic absorption and colorimetric methods using reagent-grade chemicals and Millipore water. A conventional single-compartment cell with a flat Pyrex glass window for illumination of the electrode was used in photoelectrochemical experiments. A saturated calomel electrode (SCE) with a saturated KCl agar bridge and a large-area Pt gauze electrode were used as reference and counterelectrodes, respectively.

The ac impedance studies were carried out under potentiostatic conditions using a 1255 Solartron frequency response analyzer and an 1186 Solartron electrochemical interface. A small ac signal, having 10 mV peak-to-peak amplitude at different frequencies from 0.5 to 5 kHz, modulated the electrode potential. The action spectrum was recorded using chopped light (80 Hz) and a high-intensity grating monochromator (Photon Technology International). The modulated photocurrent was detected, and the photocurrent amplitude and phase angle were determined with a PAR Model 5206 lock-in amplifier and a Tacussel-Solea Type BI-PAD potentiostat. The lamp spectrum was normalized by means of a calibrated EG&G 400 B silicon detector. Neither reflections at the cell window or electrode surface nor electrolyte absorption were taken into account.

Results and Discussion

Indium antimonide.—Electrodeposition of InSb in an unstirred bath is a diffusion-controlled process (11, 14) in which the In/Sb concentration ratio in the bath has a great influence on the composition of the electrodeposited thin film. Figure 2 shows the current *vs.* the applied potential for antimony and indium ions in citric acid solutions, respectively. It is possible to observe that diffusion limits the electrodeposition of both Sb and In from citric acid solutions and that the hydrogen overpotential depends on the cathodic process over the electrode surface. Also, stibine evolution can occur in parallel with hydrogen evolution, in the case of Sb electrodeposition.

The x-ray diffraction patterns of thin films show a dependence of their structure on the electrodeposition potential (Fig. 3). Polycrystalline hcp antimony, practically free of indium, was electrodeposited from a bath of composition 0.3M citric acid, 0.033M $InCl_3$, and 0.047M $SbCl_3$ at cathode potentials more positive than −0.60V (*vs.* SCE). At potentials ranging from −0.60 to −0.85V (*vs.* SCE), a mixture of polycrystalline fcc InSb and hcp Sb is electrodeposited, with decreasing percentages of Sb in the deposited thin films as the potential becomes more cathodic. At potentials more negative than −0.85V (*vs.* SCE), polycrystalline fcc InSb, free of In and Sb phases, was electrodeposited. InSb thin films were electrodeposited with a current efficiency higher than 85% at −0.90V (*vs.* SCE); lower

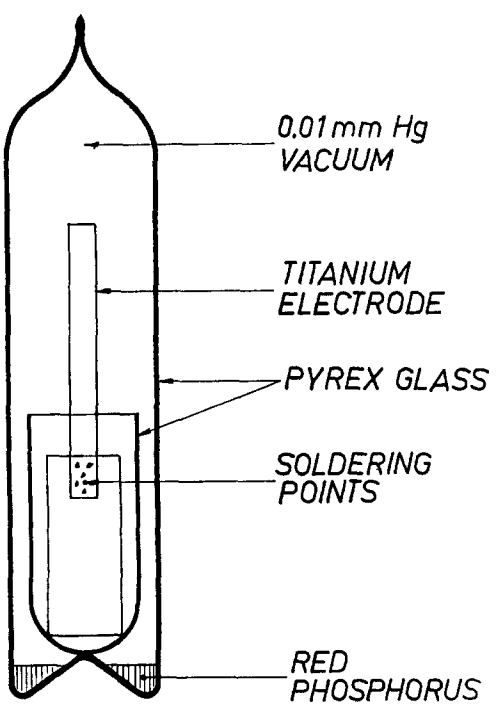

Fig. 1. Experimental phosphorization system

* Electrochemical Society Active Member.

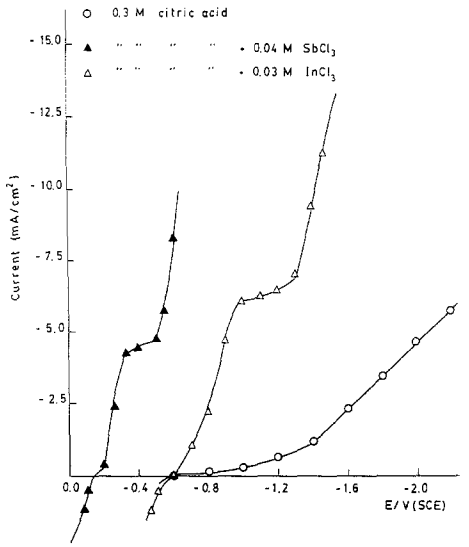

Fig. 2. Current-potential curves for In and Sb deposition from citric acid baths.

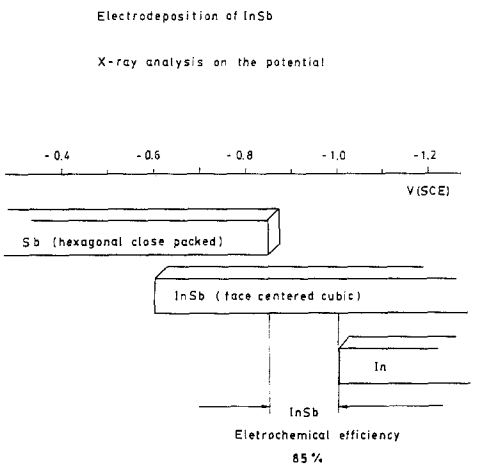

Fig. 3. Potential dependence of the x-ray structure of In-Sb films obtained by electrodeposition.

efficiencies were obtained at more cathodic potentials due to the hydrogen evolution. These films, deposited on titanium substrates, were very adherent and show the characteristic diffraction pattern of the fcc InSb phase (Fig. 4). If the potential was higher than −1.0V (*vs.* SCE), x-ray diffraction patterns showed a mixture of peaks that correspond with elemental tetragonal In and fcc InSb (Fig. 5).

Indium arsenide.—Electrodeposition of InAs from solutions that contained $InCl_3$, $AsCl_3$, and citric acid yielded different results than the electrodeposition of InSb. Figure 6 shows the current-potential curve for a 0.04*M* $AsCl_3$ and 0.3*M* citric acid solution. From the figure, due to As electroreduction potentials

$$AsO^{2-} + 4H^+ + 3e^- \rightarrow As + 2H_2O \qquad E^\circ = 0.194 \text{ V/SCE} \quad [1]$$

$$As + 3H^+ + 3e^- \rightarrow AsH_3 \qquad E^\circ = -0.843 \text{ V/SCE} \quad [2]$$

The As forms from a chemical interaction between the AsH_3 formed on the cathode and the $HAsO_2$ contained in the bath. This mechanism is similar to that proposed by Kröger (15) for CdTe. Adherent InAs thin films can be obtained on titanium at −1.40V (*vs.* SCE) from a citric bath. The as-electrodeposited InAs is amorphous and, after being annealed at 400°C for 30 min, its x-ray diffractogram showed the peaks corresponding to the InAs face-centered cubic systems, but with low crystallinity (Fig. 7).

During the electrodeposition of InAs layers, a process of photoelectrochemical activity as observed when the electrodes were illuminated with a halogen-tungsten lamp (Fig. 8). The photocathodic currents observed under illumination indicated that the grown layers showed a p-type photoconductivity.

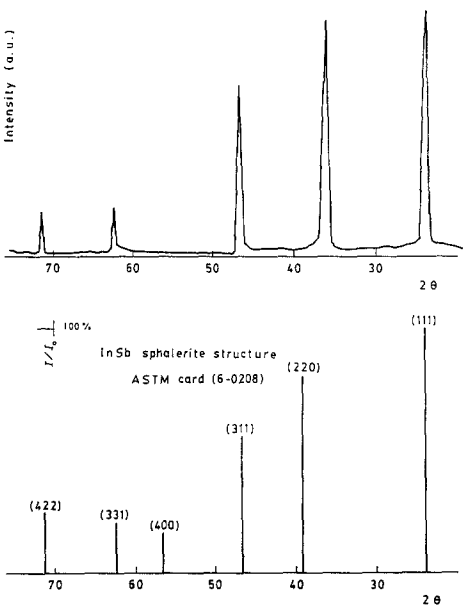

Fig. 4. X-ray diffraction pattern for an as-electroplated InSb thin film, and ASTM pattern for InSb.

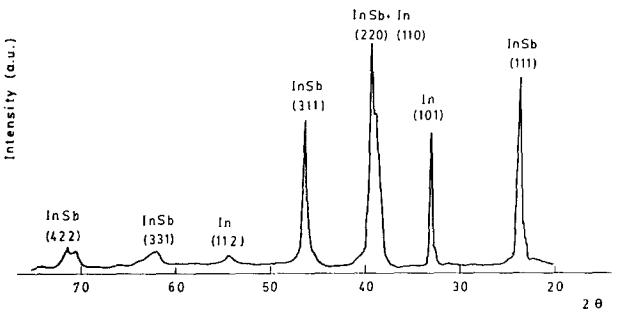

Fig. 5. X-ray diffraction pattern for an as-electroplated InSb-In alloy electroplated at −1.0V (*vs.* SCE).

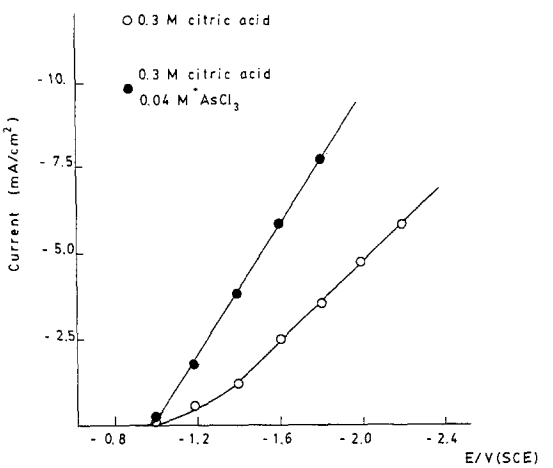

Fig. 6. Current-potential curve for As deposition from a citric bath

Indium phosphide.—Characterization of the electroplated metallic indium films after the phosphorization treatment was accomplished by x-ray diffraction. The diffractogram obtained (Fig. 9) matched literature values for InP structure (16). The pattern shows very sharp lines, indicating that the material is crystalline. No preferred orientation with respect to powder diffraction was observed. Photovoltaic activity of the prepared InP layers in a photoelectrochemical cell with an 0.5*M* HCl solution was

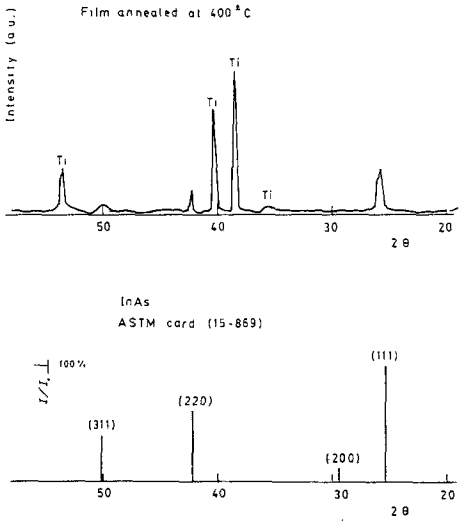

Fig. 7. X-ray diffraction pattern for an electroplated InAs thin film after annealing at 400°C, and ASTM pattern for InAs.

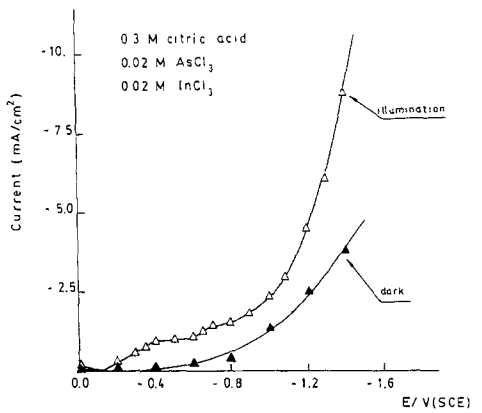

Fig. 8. Current-potential curves for InAS electrodeposition under dark and illumination.

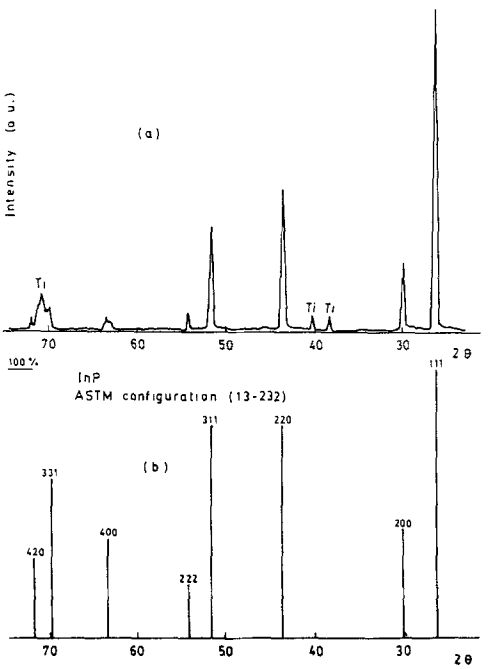

Fig. 9. X-ray diffraction pattern for an electroplated In thin film after heating in phosphorus atmosphere, and ASTM pattern for InP.

tested. Figure 10 shows the photocurrent (i_{ph})-potential behavior of an InP photoelectrode in this solution under chopped light illumination, AM1 conditions (100 mW/cm²).

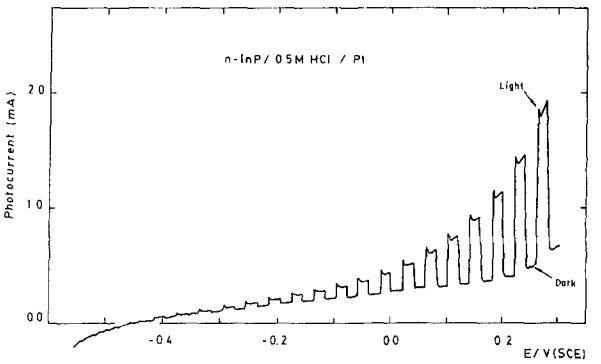

Fig. 10. Photocurrent-potential curve for n-InP with chopped white light (*ca.* 100 mW/cm²).

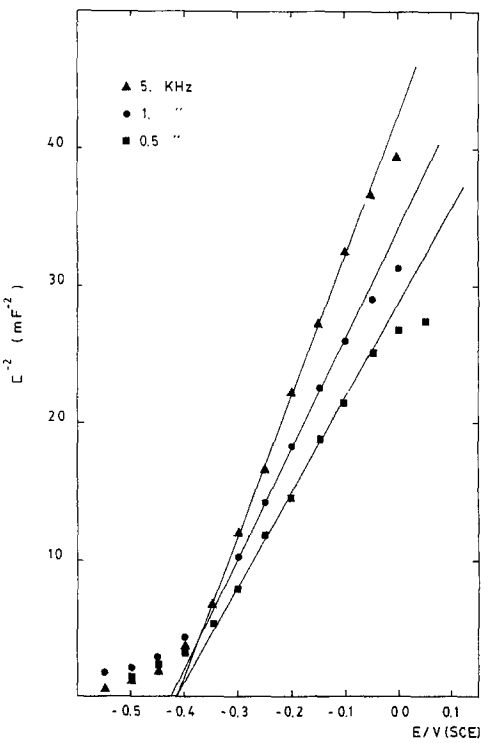

Fig. 11. Mott-Schottky plot of n-InP in 0.5M HCl at different frequenices.

The behavior in the hydrochloric solution corresponds to that of an n-type semiconductor, and electrode photocorrosion was observed. The onset of the photocurrent was just negative of −0.5V (*vs.* SCE). Notice that the i_{ph}-V curve, obtained with chopped irradiation, consists of a series of anodic current spikes. Moreover, the photocurrent did not attain a saturation value. These spiked photocurrents seen with this couple might be explained

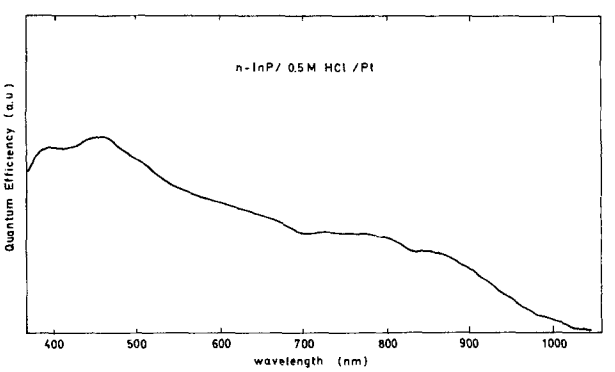

Fig. 12. Action spectra of an n-InP electrode in a HCl solution

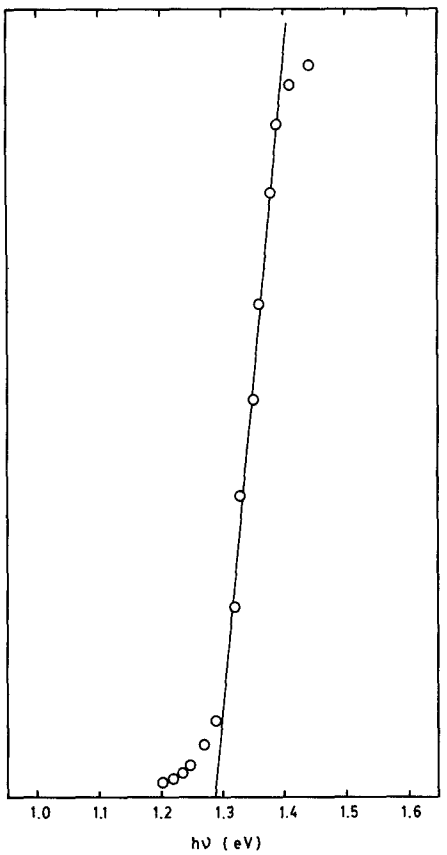

Fig. 13. Plot of $(\eta h\nu)^2$ vs. $h\nu$ for an n-InP, solution as in Fig. 12

by a process where the charge transfer competes with the electron-hole recombination over the semiconductor surface due to an ineffective separation of the electron-hole pairs (17-18).

Mott-Schottky plots ($1/C^2$ *vs.* applied potential, where C is the capacitance) for n-InP samples in 0.5 HCl are shown in Fig. 11. The plots show linear behavior in a range of potentials for the investigated frequencies. Although there was some frequency dispersion in the plots, estimates of the flatband potential (V_{FB}) can be obtained. The intercept with the potential axis gives a value of $V_{FB} = -0.42$V (*vs.* SCE). Frequency dispersion in the capacity measurements has often been observed in the literature (19). Possible causes are the contribution of the bulk of the electrode and/or nonuniform ac current distribution due to irregularity of the electrode surface. The photocurrent onset for n-InP thin films occurs at potentials more negative than the V_{FB} determined from capacitance measurements. However, photocurrent onsets may not be reliable for estimates of bandedge energies, *e.g.*, because of recombination effects or because filling of surface states by electrons while the photoanode is under illumination can cause the bandedges to shift to more negative values (20).

The photocurrent action spectrum of an n-Inp electrode in the same electrolyte is shown in Fig. 12. The bandgap of InP can be determined from the $(\eta h\nu)^2$ *vs.* $(h\nu)$ plot (for a direct transition) near the bandedge region [21-22]. η here is the quantum efficiency, proportional to i_{ph}, and $h\nu$ is the photon energy. As shown in Fig. 13, a $(\eta h\nu)^2$ *vs.* $(h\nu)$ plot gives a fairly good straight line. The intercept with the x-axis gives an energy gap of 1.29 eV, in agreement with the usual values given in the literature (1).

Conclusions

InSb and InAs can be grown by direct electroplating. While as-deposited InSb thin films are crystalline, InAs layers show low crystallinity, even after annealing at 400°C. During the electrodeposition of InAs layers, photoelectrochemical activity is observed. InP thin films can be prepared by phosphorization of electroplated indium layers in a phosphorus atmosphere. The films were identified by x-ray diffraction to be InP in the sphalerite phase of good crystalline quality. Photoelectrochemical activity of InP films was tested in a HCl solution where the photoconductivity of prepared films was n-type. The physical parameters E_g and V_{FB} were also obtained in this electrolyte.

Acknowledgments

We thank Dr. Bayon for his x-ray facilities. Technical assistance by E. Galiano is gratefully acknowledged. The Spanish Ministry of Industry and Energy has supported this research by means of the Instituto de Energías Renovables (CIEMAT).

Manuscript submitted July 29, 1988; revised manuscript received March 24, 1989. This was Paper 375 presented at the Chicago, IL, Meeting of the Society, Oct. 9-14, 1988.

Instituto de Energias Renovables (CIEMAT) assisted in meeting the publication costs of this article.

REFERENCES

1. A. Yamamoto, M. Yamaguchi, and C. Hemura, *Appl. Phys. Lett.*, **47,** 9751 (1985).
2. A. Heller, B. Millet, and H. J. Lewerenz, *Phys. Rev.*, **102,** 6555 (1980).
3. E. Aharon-Shalom and A. Heller, *This Journal*, **129,** 2865 (1982).
4. B. Miller, *ibid.*, **131,** 91 (1984).
5. A. Darkowski and M. Cocivera, *ibid.*, **134,** 226 (1987).
6. R. K. Pandey and A. J. N. Rooz, *J. Phys. D. Appl. Phys.*, **19,** 917 (1986).
7. F. Mondon, *This Journal*, **132,** 319 (1985).
8. R. T. Green, D. K. Walker, and C. M. Wolfe, *ibid.*, **133,** 2278 (1985).
9. A. B. Ellis, J. M. Bolts, and M. S. Wrigton, *This Journal*, **134,** 1603 (1987).
10. I. G. Diuom, J. Vedel, and B. Tremillon, *J. Electroanal. Chem.*, **139,** 329 (1982).
11. Y. N. Sadana and J. P. Sinhg, *Plat. Surf. Fin.*, **12,** 64 (1985).
12. J. Herrero and J. Ortega, *Solar Energy Mat.*, **16,** 477 (1987).
13. J. Herrero and J. Ortega, *ibid.*, **17,** 357 (1988).
14. T. Okubo and M. Landau, Abstract 376, p. 547, The Electrochemical Society Extended Abstracts, Vol. 88-2, Chicago, IL, Oct. 9-14, 1988.
15. F. A. Kröger, *This Journal*, **125,** 2028 (1978).
16. ASTM Card 13-232 (1983).
17. T. H. Wilson, *This Journal*, **127,** 228 (1980).
18. P. Salvador, *J. Appl. Phys.*, **55,** 2977 (1987).
19. S. Piazza and H. Tributsch, *J. Appl. Electrochem.*, **17,** 613 (1987).
20. S. Cooper, J. A. Turner, B. A. Parkinson, and A. J. Nozik, *J. Appl. Phys.*, **54,** 6463 (1983).
21. W. W. Gärtner, *Phys. Rev.*, **116,** 84 (1959).
22. M. A. Butler, *J. Appl. Phys.*, **48,** 1914 (1977).